ANALYSIS OF KINEMATCIS AND HEAD INJURY MECHANNISMS IN CAR TO CHILD CYCLSIT COLLISION SIMULATION USING HUMAN FINITE ELEMENT MODEL

Tadasuke Katsuhara
Yasuo Yamamae
Tsuyoshi Yasuki
Toyota Motor Corporation
Japan

Hiroyuki Umetani
Toyota Systems
Japan

Paper Number 19-0030

ABSTRACT

According to the traffic accident data in Japan [1], the third largest number of fatalities is due to collision between car and cyclist. Head injuries are the most frequent cause of cyclist fatalities. Head injury risk depends on the stiffness of the head collision location of the vehicles. The collision location of a child's head is different from that of an adult's head in a traffic accident. Therefore, there is benefit of examining the injury mechanism of child cyclists for safety equipment.
In this study, a total of 400 cases of car-to-cyclist collision were simulated by varying car speed, bicycle speed and initial position of collision using child and adult human Finite Element (FE) models and the head injury mechanisms were analyzed by investigating the kinematics and the kinetics of child and adult cyclists. The THUMS Version 4 Ten Years Old (10YO) model was used for the child cyclist and the THUMS Version 4 American Mail 50%tile (AM50) model for the adult cyclist. The bicycle FE model of a city cycle was established bicycle. The occurrence risk of skull fracture and Diffuse Axonal Injury (DAI) was investigated in 10YO and AM50 cyclists. In 10YO, approximately 90 % of the head contact points were distributed on the car body and 10 % was distributed on the ground. In AM50, the head contact points on the ground accounted for approximately 30 %, 70 % were distributed on the car body.
It was found that the skull fracture and DAI occurrence were predicted in the 10YO when the head contacted the car hood in the car speed of 30 km/h or more. The impact velocity of the upper body was increased by contacting between the pelvis and the front edge of the car hood. As a result, head impact velocity and rotational velocity became high after the shoulder contacted the hood. In the AM50 whose pelvis rode on the hood, the upper body fell down toward the hood gradually. As a result, the skull fracture occurred when the head contacted the A-pillar in the car speed of 40 km/h or more, which was lower than that in the 10YO. In the case which bicyclists head contacted a ground after car collision, the skull fracture was predicted even in the car speed of 10km/h. The DAI occurrence was not predicted.

INTRODUCTION

According to the data collected by the Ministry of Internal Affair and Communications Statistics Bureau [2], 30 % of traffic accident fatalities involving children 14 years old and under. According to the statistical data of the National Police Agency in Japan [1], traffic accident fatalities of child cyclists under 15 years old is the third highest, preceded by pedestrians and car occupants. The authors have already studied the injury mechanisms of both child pedestrians [3] and child occupants [4]. In this study, the authors investigated injury mechanisms on child cyclists.
Recently cars which are equipped with the Automatic Emergency Brake (AEB) have been sold in Japan. When all cars are equipped with AEB, it is expected that the collision speed will reduce and the risk of cyclist injury will decrease during the cars collide to cyclists. However, the fatality risk will remain if the cyclists collides with the ground after a car-to-cyclist collision. In this study, not only head-to-car contact but also head-to-ground contact after car collision will be analyzed.
To analyze cyclist collision kinematics and injuries, physical tests using Anthropomorphic Test Devices (ATD) [5], [6] and simulation using MADYMO [7], [8] and human Finite Element (FE) models [9], [10] were

conducted. Maki et al. [7] studied traffic accident statistics and clarified the cyclist's kinematics after car collision using MADYMO. Omoda et al. [8] simulated ground contact of cyclists after car collision using MADYMO and indicated that the head injury risk of cyclist's head to ground was higher than that of head to car. Mizuno et al. [10] studied the difference of the kinematics after collision between pedestrians and cyclists using human FE models. Moreover, A-pillar to cyclist head with helmet collisions were simulated and the effect of the helmet was clarified. The brain injury such as Diffuse Axonal Injury (DAI) cannot be directly simulated using ATD and MADYMO, while human FE model with detail brain model is available to analyze DAI.

To simulate a real traffic accident, various collision conditions need to be considered. In this study, a total of 200 cases of car-to-child cyclist collisions based on the real traffic accident were simulated by using the human FE model representing a child cyclist in order to clarify the mechanisms of skull fracture and DAI for head to car and head to ground contact. For comparison, the car-to-adult cyclist collisions also were simulated in the same conditions as the child cyclist.

METHOD

Car and Ground Models

The FE car model was the same as used in a previous study [11] as shown in Figure 1. A sedan was selected as the car type. Rigid materials were assumed for the engine and deformable material was assumed for the other parts. The tires and the steering could rotate. The ground was assumed to be a rigid plane.

Figure 1.Car and ground FE models

Cyclist Model

The age of the cyclist was chosen to be 10 years old. The THUMS Version 4 10YO occupant model was used for the child cyclist (Figure 2). Bicycle type was a city cycle. A twenty two inches tire size bicycle was used for the child cyclist. The height of bicycle saddle was 0.7 m from the ground. The head height of the seated child cyclist was 1.35 m and his weight was 34.0 kg. The THUMS Version 4 AM50 occupant model was used for the adult cyclist. A twenty six inches tire size bicycle was used for the adult cyclist. The height of bicycle saddle was 0.9 m from the ground. The head height of the seated adult cyclist was 1.70 m and his weight was 77.0 kg. The friction coefficient between cyclists and the car was 0.3, for the ground was 0.7.

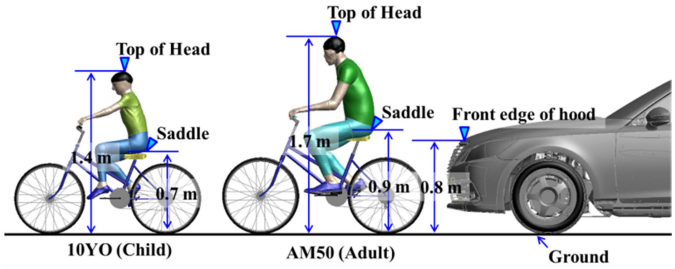

Figure 2. 10YO (Child) and AM50 (Adult) cyclist FE models

INJURY INDICIES AND CRITERIA

In this study, risk of the skull fracture and DAI were evaluated. HIC_{15} was used as an index of skull fracture in order to facilitate comparison with other studies. It was postulated that skull fracture (AIS3+, 30% probability) occurred when HIC_{15} exceeded 700 [12]. DAI was estimated using the cumulative strain damage measure (CSDM) proposed by Takhounts et al. [13]. CSDM is an index used to assess the occurrence of DAI based on the volume ratio of distortion areas in the brain exceeding a threshold value (25 %) with respect to the volume of the whole brain. According to the brain injury risk curve derived by Takhounts et al. [14], a CSDM value of 49 % was equivalent to a 50 % probability of DAI (AIS4+).

SIMULATION CONDITION

The simulation condition was shown in Table 1. The parameters were car speeds, bicycle speeds and initial impact positions. The car speed was changed from 10 km/h to 50 km/h at an interval of 10 km/h. The bicycle speed was changed from 5 km/h to 25 km/h at an interval of 5 km/h. The initial impact position of cyclist was changed from 1000 mm to - 400 mm based on cyclist head center of gravity at an interval of 200 mm as shown in Figure 3. A total of 400 cases were simulated in each 10YO and AM50. A number of 10YO cases were 200 cases (from Case 1 to Case 200). A number of AM50 cases also 200 cases (from Case 201 to Case 400).

Table 1. Simulation Conditions

Parameter	Variation							
Cyclist	THUMS Version 4 10YO (Child)				THUMS Version 4 AM50 (Adult)			
Bicycle tire size [inches]	22				26			
Car type	Sedan							
Car speed [km/h]	10	20	30	40	50			
Bicycle speed [km/h]	5	10	15	20	25			
Initial impact position [mm]	1000	800	600	400	200	0	-200	-400
Total Case	400 Cases							

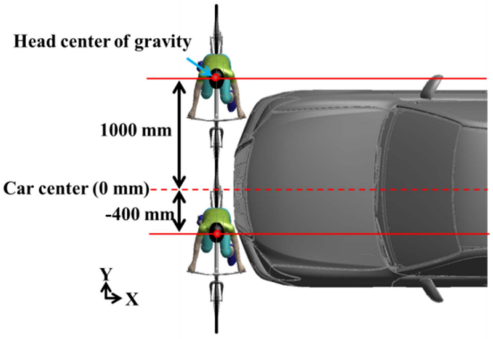

Figure 3. Definition of initial impact position

RESULTS

Distribution of HIC_{15} and CSDM

The distributions of HIC_{15} and CSDM are shown in Figure 4. Blue areas show the case which cyclist head contacted the car body. Red areas show the case which cyclist head contacted the ground. Based on the criterion of both HIC_{15} (700) and CSDM (49 %), all results were divided into three categories as follows (A, B, C). Category A are cases in which both HIC_{15} and CSDM are equal to and over their criteria (HIC_{15} 700, CSDM 49%). Category B are cases that only HIC_{15} is equal to and over the criterion. Category C are cases in which both HIC_{15} and CSDM are less than the criteria. For the 10YO cases, Category A for head car contact and head ground contact were 18 % and 0.5 % respectively. Category B for head car contact and head ground contact were 35 % and 9 % respectively. For the AM50 cases, Category A did not occur both head car and head ground contact cases. Category B in head car contact case was 12% and 18 % for head ground contact case.

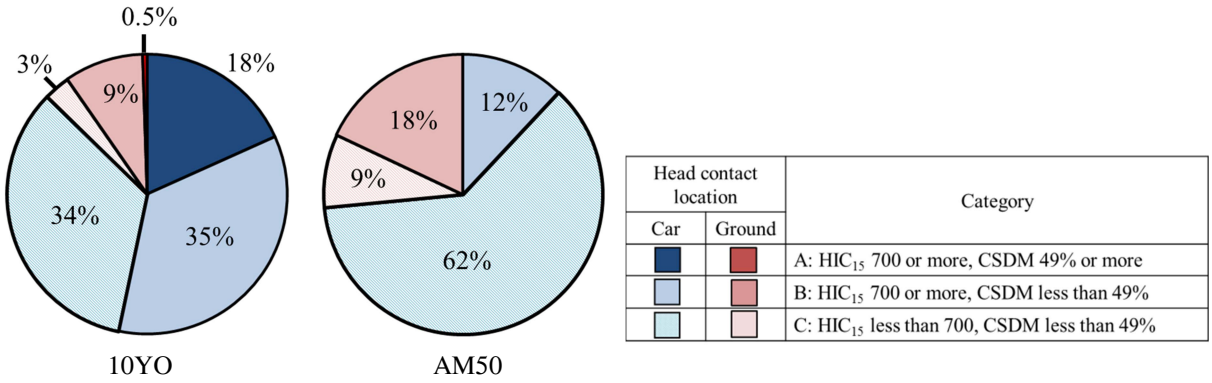

Figure 4. Distribution of HIC_{15} and CSDM of 10YO and AM50 cyclists

Relationship between head contact points and HIC_{15} is investigated as shown in Figure 5. Solid circles show the head contact points. Their color indicates the HIC_{15} level; red is $HIC_{15} \geq 700$ (skull fracture probability 30 %), yellow is $700 > HIC_{15} \geq 500$, green is $500 > HIC_{15} \geq 300$ and blue is $300 > HIC_{15}$. In 10YO of head car contact case, red solid circles ($HIC_{15} \geq 700$) distributed on the car rearward of the hood and the A-pillar while the blue solid circles distributed on the car front side of the hood. In 10YO of head ground contact case, most of head contact points show red color.

In AM50 of head contact case, red solid circles distributed on the A-pillar. The contact points of both hood and windshield show blue or green color. In also AM50 of head ground contact case, most of head contact points show red color.

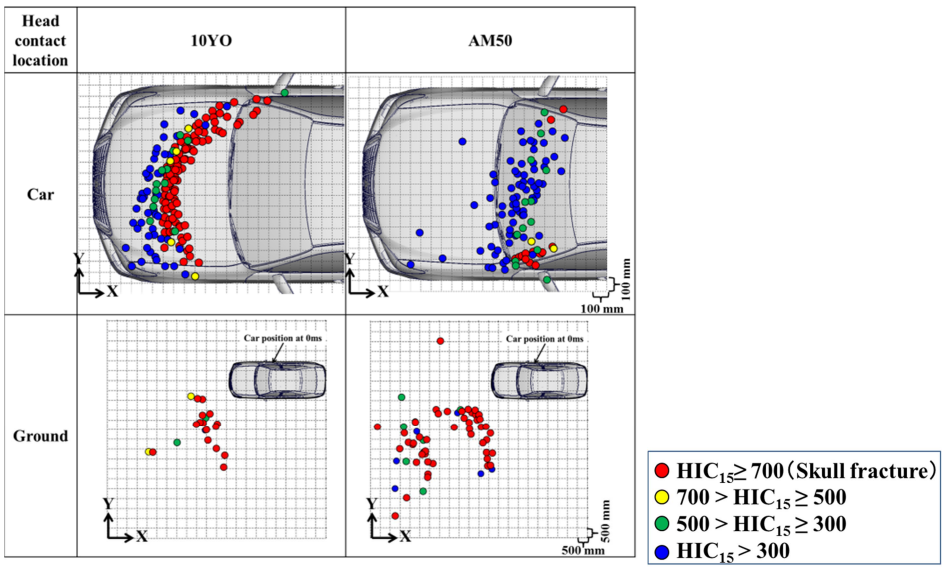

Figure 5. Distribution of head contact points with HIC_{15} levels

Relationship between head contact points and CSDM is investigated as shown in Figure 6. Solid circles show the head contact points. Their color indicates the CSDM revel; red is CSDM ≥ 49 % (DAI probability 50%), yellow is 49 % > CSDM ≥ 30 %, green is 30 % > CSDM ≥ 10 % and blue is 10 % > CSDM. In 10YO of head car contact case, red and yellow solid circles, which indicated high risk of DAI, were shown in the car rearward of the hood and A-pillar while green and blue solid circles distributed on the car front side of the hood. In 10YO of head ground contact case, red and yellow solid circles were shown in the furthermore from the car. In AM50 of head car contact case, there was no case which was over 30 % of CSDM. Most of cases were less than 10% of CSDM. In also AM50 of head ground contact case, there was no case which exceeded 49 % of CSDM.

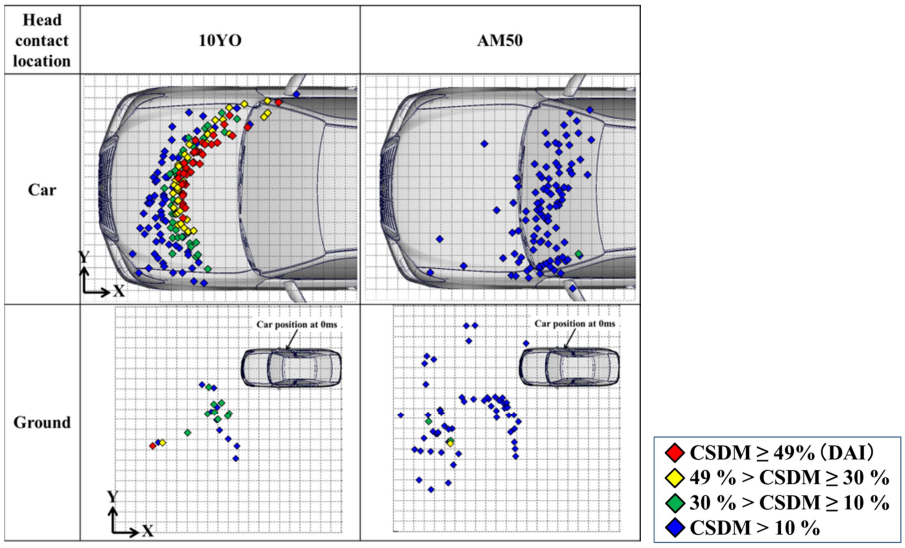

Figure 6. Distribution of head contact points with CSDM levels

Relationship between Car Speeds and Head Injury Indices (HIC_{15}, CSDM)

The relationship between car speeds and HIC_{15} is shown in Figure 7. In head car contact cases of both 10YO and AM50 cyclist, higher the car speeds were, the higher $HIC_{15}$was. At the car speed of 30 km/h, half of 10YO cases were over the criteria. On the other hand, only one case was over the criteria in AM50 cases. In head ground contact cases of both 10YO and AM50 cyclists , HIC_{15} in low car speed cases (10, 20, 30 km/h) were higher than that in high car speed cases (40, 50 km/h).

The relationship between car speed and CSDM was shown in Figure 8. In head car contact cases of both 10YO and AM50 cyclists, CSDM also was high with increasing car speed. In the 10YO, CSDM exceeded the criterion in car speed of 30 km/h or more. In the AM50, CSDM was lower than 10 %. In head ground contact cases, a correlation between CSDM and car speed was not found in either the 10YO and AM50 cases.

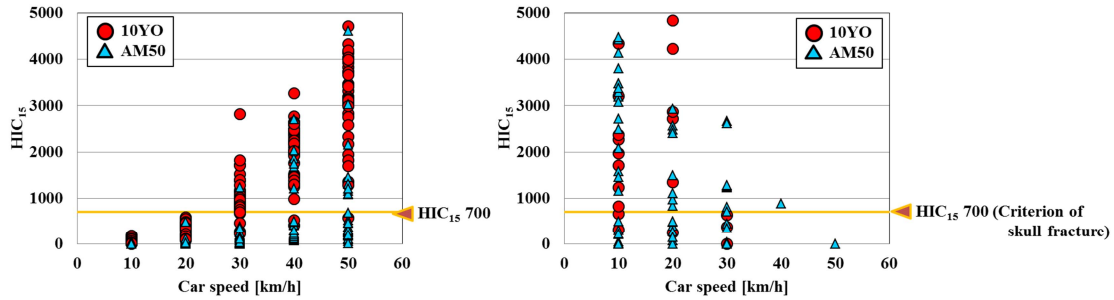

Car contact Ground contact

Figure 7. Relationship between car speed and HIC_{15} of 10YO and AM50 cyclists

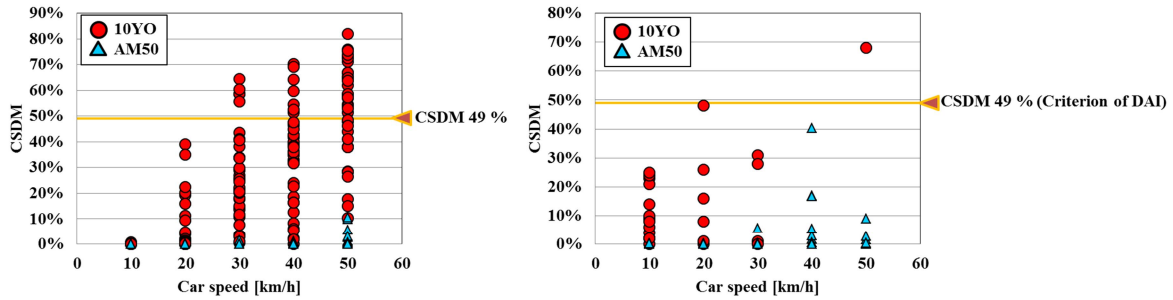

Car contact Ground contact

Figure 8. Relationship between car speed and CSDM of 10YO and AM50 cyclists

Relationship between Head Impact Velocities and HIC_{15}

The relationship between head impact velocity and HIC_{15} was shown in Figure 9. In head car contact cases, HIC_{15} became high in proportion to head impact velocities. Head impact velocities in AM50 cases trended to be lower than those of the 10YO cases. In head ground contact cases, HIC_{15} tended to be high in both 10YO and AM50 cases even though head impact velocity was low (between 5 m/s and 8 m/s).

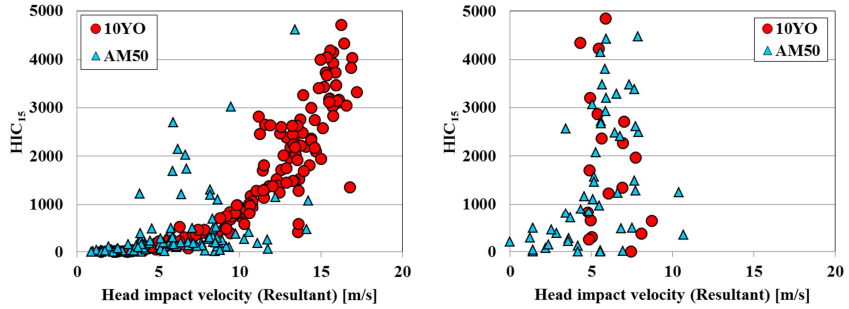

Car contact Ground contact

Figure 9. Relationship between head impact velocities and HIC_{15} of 10YO and AM50 cyclists

Relationship between Head Rotational Velocities, Accelerations and CSDM

The relationship between head rotational velocity and CSDM was shown in Figure 10. In head car contact cases of 10Y cyclist, CSDM became high in proportion to head rotational velocities. In AM50 cyclist, CSDM was low in all head rotational velocities. Regarding head ground contact cases of 10YO and AM50 cyclists, CSDM was similar to zero between head rotational velocity of 0 and 50 rad/s. From head rotational velocity 50 rad/s, CSDM increased up to 50%. The relationship between head rotational accelerations and CSDM was shown in Figure 11. In head car contact case of 10YO, head rotational acceleration was higher than that in AM50 cases. CSDM in 10YO also was higher than that in AM50.

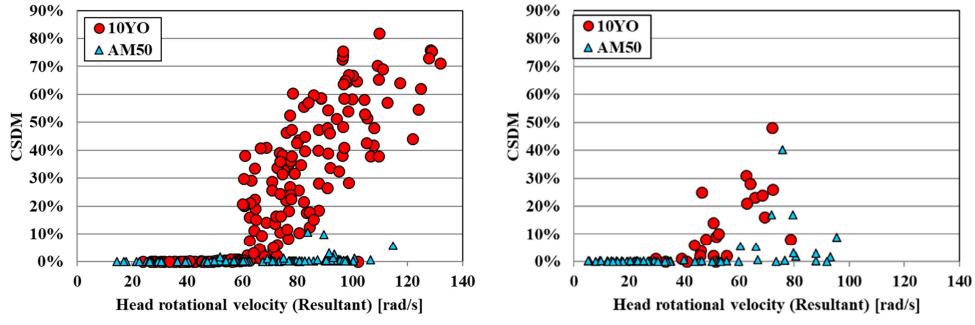

Car Contact Ground Contact

Figure 10. Relationship between head rotational velocities and CSDM of 10YO and AM50 cyclists

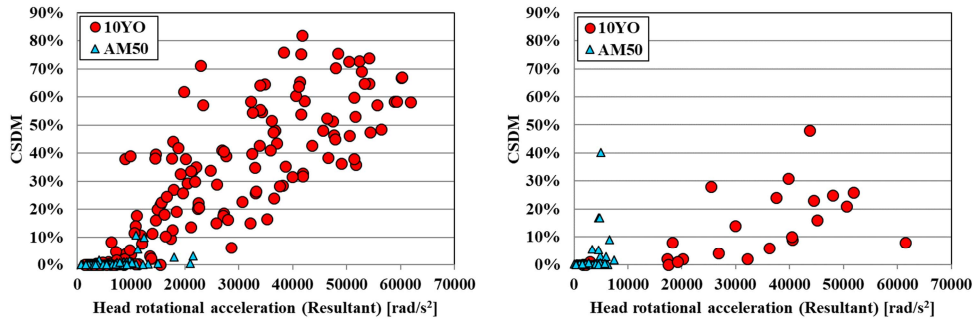

Figure 11. Relationship between head rotational accelerations and CSDM of 10YO and AM50 cyclists

Kinematics of a Car Contact Case

As an example of the case which cyclist head contacted the car body, the results of Case 119 (10YO) and Case 319 (AM50) were shown in Table 3. The collision conditions of both cases were car speed: 40 km/h, bicycle speed: 10 km/h and initial impact position: 200 mm. HIC_{15} was 2261 and CSDM was 55.5 % in Case 119 when 10YO head contacted the hood. HIC_{15} was 2034 and CSDM was 0.5 % in Case 319 when AM50 head contacted the A-pillar. The kinematics of 10YO and AM50 were shown in Figure 12 and 13. In the upper view, 10YO obliquely moved toward the car rearward and his head collided to the hood. On the other hand, AM50 obliquely moved to car rearward on the car hood and his head contacted to A-pillar. In the lateral view, 10YO lower leg and the thigh contacted the gill at 10 ms. At 20 ms, the pelvis contacted the front edge of the hood. At 30 ms, the upper body started to fall down toward the hood. At 60 ms, the shoulder contacted the hood. Finally, the head contacted the hood at 80 ms. In AM50 case, the lower leg contacted the grill at 10 ms and AM50 thigh contacted the hood at 20 ms. At 30 ms, his pelvis ridded on the hood and his upper body moved toward the car rearward. His upper body fell down toward the hood and his head contacted the lower parts of A-pillar at 170 ms.

Table 3. Head injury results in head car contact cases

Case No.	Bicyclist	Collision condition			Head impact location	HIC_{15}	CSDM
		Car speed	Bicycle speed	Impact position			
Case 119	10YO	40 km/h	10 km/h	200 mm	Hood	2216	55.5 %
Case 319	AM50				A-Pillar	2034	0.5 %

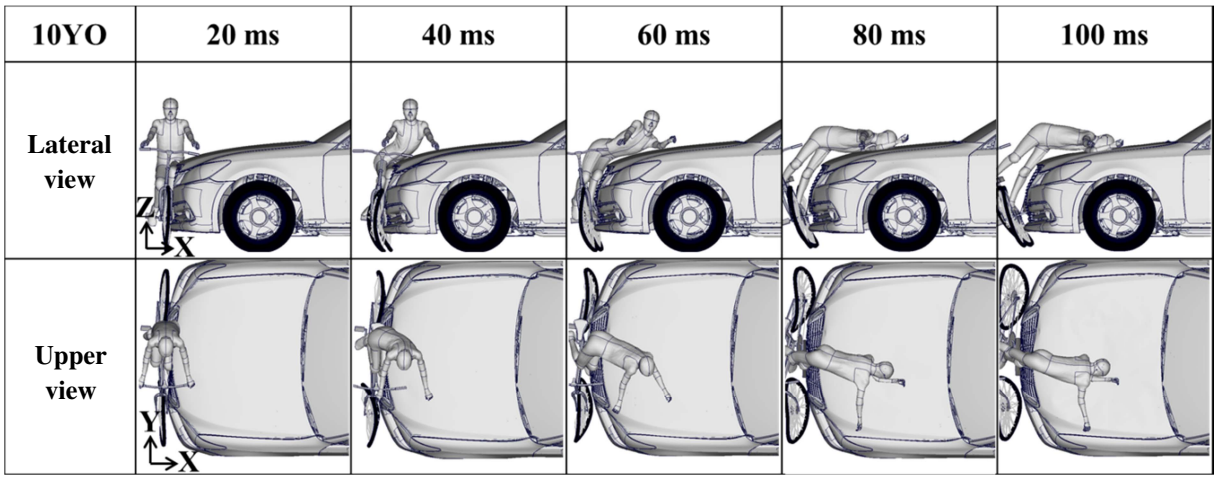

Figure 12. Kinematics of 10YO (Case 119) cyclist during impact

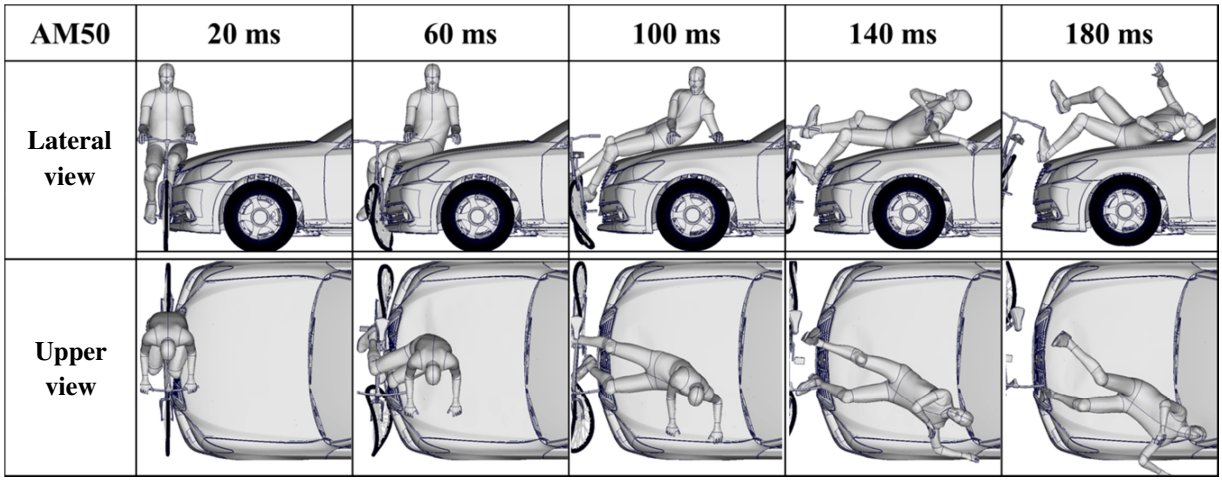

Figure 13. Kinematics of AM50 (Case 319) cyclist during collision

Kinematics and Kinetics of a Ground Contact Case

As an example of the case which cyclist head contacted the ground, the results of Case 149 (10YO) and Case 349 (AM50) were shown in Table 4. The collision conditions of Case 149 and Case 349 were car speed: 10km/h, bicycle speed: 25 km/h and initial impact position: 0mm (Car center). In Case 149 (10YO), HIC_{15} indicated 2268 and CSDM was 0.0 %. In Case 349 (AM50), HIC_{15} was 4606 and CSDM was 0.1%. As shown in Figure 14 and 15, the kinematics of Case 149 (10YO) was similar to that of Case 349 (AM50). Upper body of cyclist fell down toward the ground after car-to-bicycle collision. At first, lower legs contacted the ground and cyclists fell down toward the ground from their head. As a result, Z direction of head impact velocity in both cases decreased gradually and their head impacted at 6 m/s of head impact velocity (Figure 16). Head rotational velocity was approximately 10 rad/s before head contacted the ground (Figure 17). After head contacted the ground, head rotational velocity increased gradually to 60 rad/s. As a result, head rotational acceleration increased to 5500 rad/s^2.

Table 4. Head injury results in head ground contact cases

Case No.	Bicyclist	Collision condition			Head impact location	HIC_{15}	CSDM
		Car speed	Bicycle speed	Impact position			
Case 149	10YO	10 km/h	25 km/h	0 mm	Ground	2268	0.0 %
Case 349	AM50				Ground	4606	0.1 %

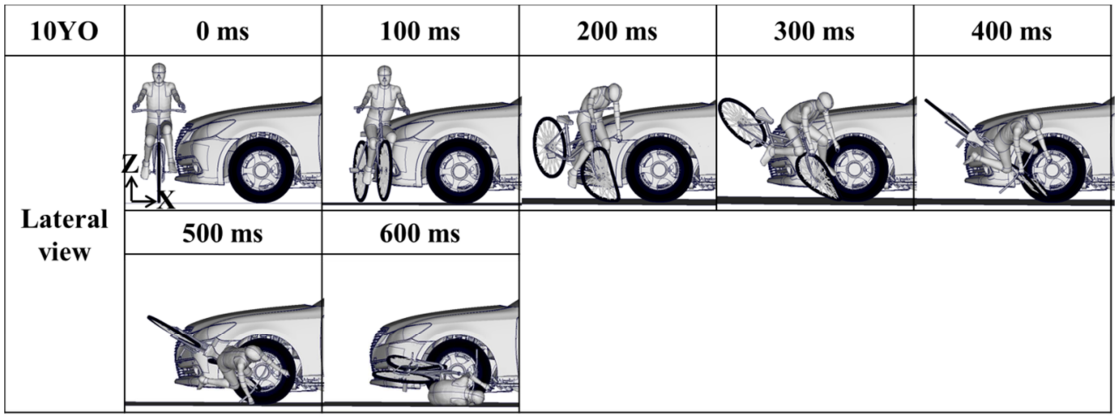

Figure 14. Kinematics of 10YO (Case 149) cyclist during collision

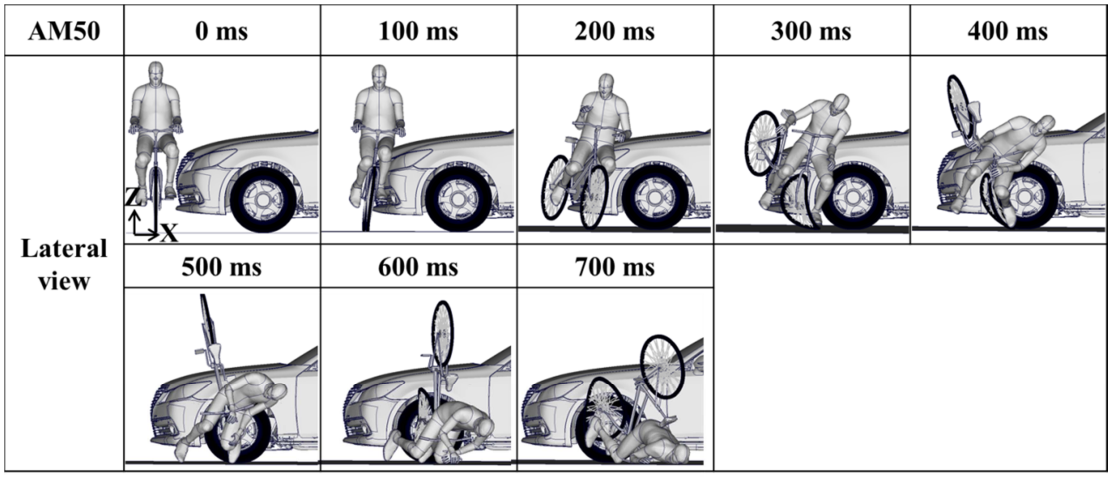

Figure 15. Kinematics of AM50 (Case 349) cyclist during collision

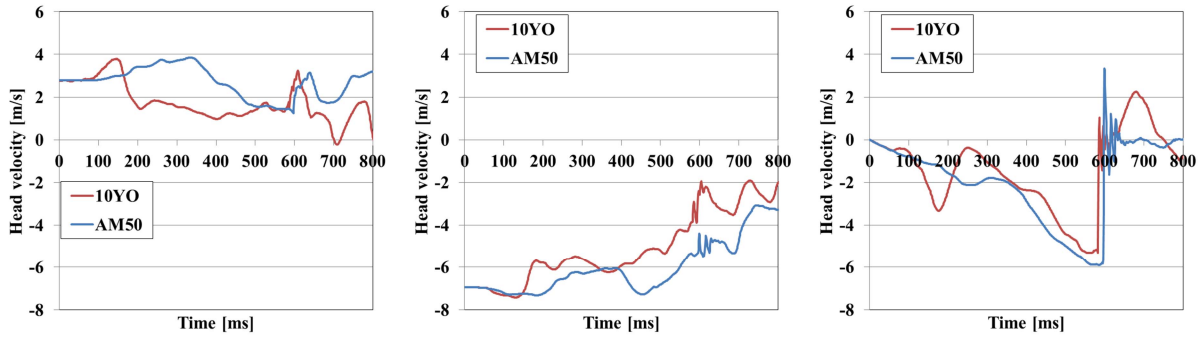

X direction Y direction Z direction

Figure 16. Head impact velocity of 10YO and AM50 cyclists

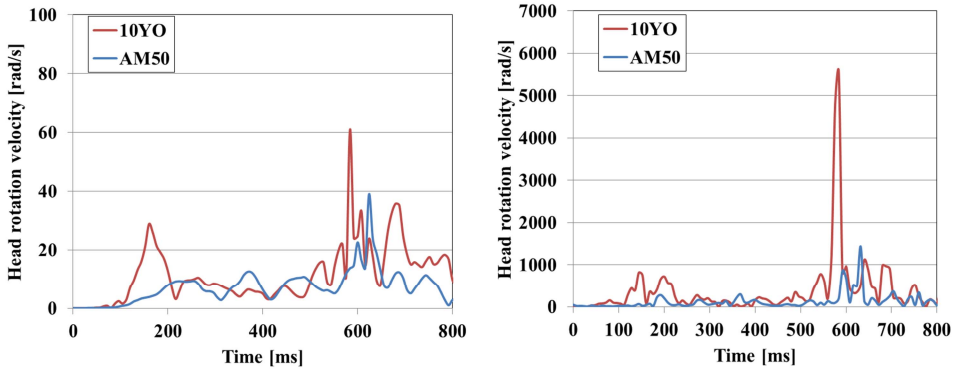

Rotational velocity Rotatonal acceleration

Figure 17. Head rotational velocity and rotational acceleration of 10YO and AM50 cyclists

DISCUSSION

A total of 400 cases of car-to-cyclist collision were simulated by using THUMS Version 4 10YO and AM50 models and the relationship between car speed and head injury (skull fracture, DAI) risk was investigated in 10YO and AM50 cyclists. In AM50 cyclist, the skull fracture was predicted when the head contacted the A-pillar in the car speed 40 km/h or more. On the other hand, the skull fracture and DAI were predicted in 10YO cyclist when head contacted the hood or A-pillar in the car speed 30 km/h or more. In the case which head contacted the ground, the skull fracture mostly occurred in both 10YO and AM50 cyclists even in the car speed 10 km/h while DAI was not predicted.

Relationship between Car Speed and HIC_{15}/CSDM

Both HIC_{15} and CSDM in 10YO cyclist exceeded their criteria when cyclist head contacted the hood or A-pillar at the car speed 30 km/h or more. Head impact velocity, rotational velocity and kinematics in 10YO cyclist were compared between car speed of 20 km/h and 30km/h as shown in Table 5. At the car speed 30 km/h (Case 68), head impact velocity was 11.4 m/s while head impact velocity was 8.3 m/s at the car speed 20 km/h (Case 67). As shown in Figure 9, high HIC_{15} values at the car speed 30 km/h were seemingly caused by high head impact velocity. The kinematics between the car speed 20 km/h (Case 67) and 30 km/h (Case 68) were compared as shown in Figure 18. The cyclist kinematics of car speed 30 km/h was similar to that of 20 km/h. Cyclist pelvis contacted the front edge of the car hood and cyclist head contacted the hood after shoulder contact. However, the contact timing of car speed 30 km/h case was higher than that of 20 km/h case. It was seemingly due to the difference of pelvis contact force. In car speed of 30 km/h case, cyclist pelvis was forcibly pushed away. As a result, cyclist upper body fell down and head rotated around shoulder rapidly. As a result, head translational velocity became high. Head rotational velocity also became high and high head rotational acceleration was generated when cyclist head contacted the hood. As a result, brain strain increased and exceeded 25 %. As shown in Figure 19, the higher pelvis contact forces were the higher head contact forces were in 10YO cyclist cases. On the other hand, the pelvis contact force in AM50 was not in proportion to the head contact force. It was due to AM50 pelvis riding on the hood.

Table 5.Comparison 10YO results between car speed of 20 km/h and 30km/h

Case No.	Bicyclist	Collision condition			Head impact location	Head impact velocity	Maximum head rotational acceleration	HIC_{15}	CSDM
		Car speed	Bicycle speed	Impact position					
Case 67	10YO	20 km/h	20 km/h	600 mm	Hood	8.3 m/s	7000 rad/s²	486	22 %
Case 68		30 km/h	20 km/h	600 mm	Hood	11.4 m/s	13000 rad/s²	1703	60 %

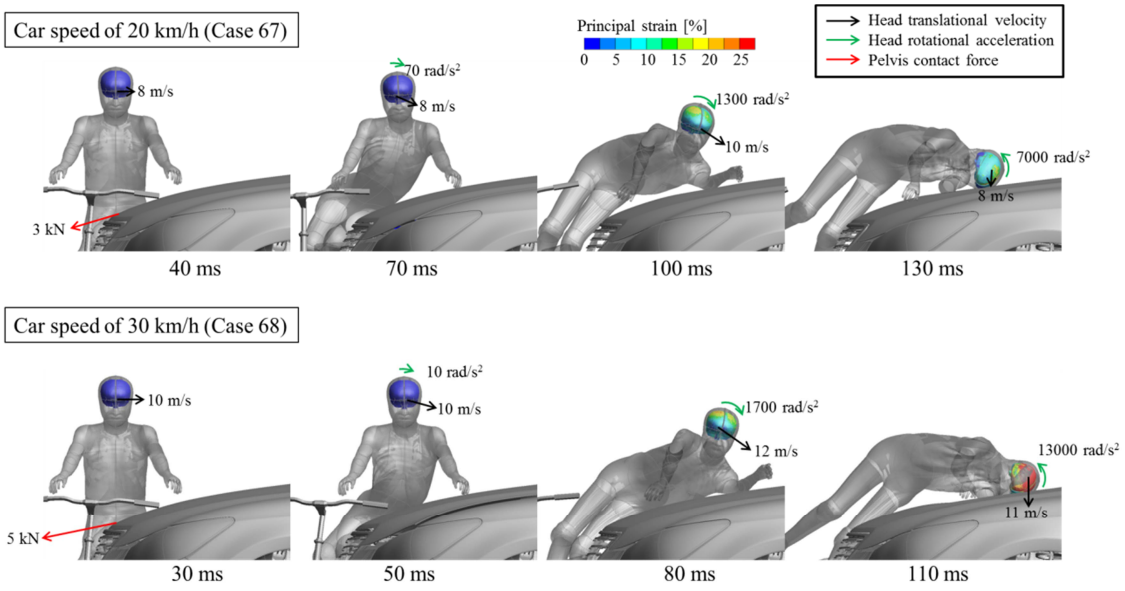

Figure 18. Comparison of kinematics, brain strains, head velocities and pelvis contact forces in 10YO bicyclist between car speed 20 km/h and 30 km/h

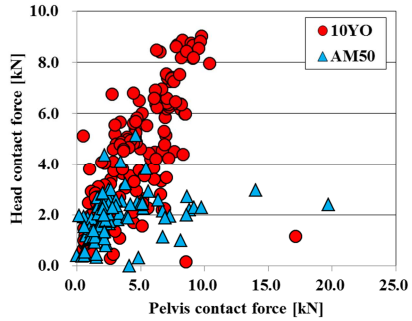

Figure 19. Relationship between head contact force and pelvis contact force

Head Injury Risk in Ground Contact Cases

In the case which head contacted the ground, the risk of skull fracture was high in 10YO and AM50 cyclists at the low car speed. As shown in Figure 16, Z direction of head impact velocity in both 10YO and AM50 monotonically decreased and head impacted the ground at approximately 6 m/s. As a result, HIC_{15} indicated 2268 in 10YO and 4606 in AM50. Matsui et al. [15] reported that HIC_{15} indicated 6525when an head impactor fell down toward a concrete ground from 1.5 m height (Head impact velocity: 5.4 m/s). HIC_{15} exceeded the criterion of skull fracture (700) in the results of both our study and Matsui's study.

CSDM in both 10YO and AM50 cyclists indicated the low value (under 49%). Low CSDM was seemingly attributed to the small head rotation. As an example of the case which head contacted the ground, AM50 cyclist case (Case 349) was shown in Figure 18. The large head rotation did not occurred when head contacted the ground. As a result, brain strain did not exceed 25 % at 670 ms.

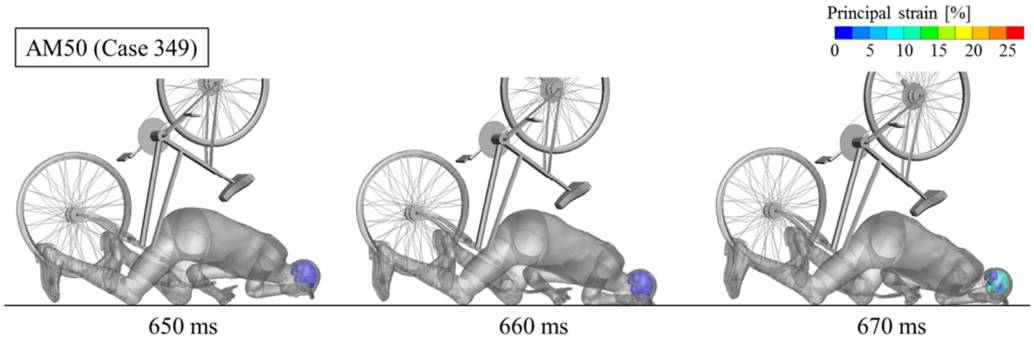

Figure 20. Kinematics and brain strain of cyclist in head ground contact case

LIMITATION

In this study, assumptions for car-to-child cyclist collision was used. In an actual car-to-cyclist accident, various collision directions, car types, bicycle types, cyclist ages are involved. The results of this research are not intended to represent all cyclist accident. Countermeasure development based on this research may not match intention when the car or bicycle types are different than those in this study. In the future, more research which takes these differences into account will be necessary.

CONCLUSIONS

A total of 400 cases of car-to-cyclist collision were simulated by using THUMS Version 4 10YO and AM50 FE models, and the relationship between car speed and skull fracture/DAI was investigated. It was found that the risk of skull fracture and DAI in the AM50 cyclist was reduced if the car speed was restrained to 30km/h. On the other hand, the car speed which reduced the skull fracture and DAI risk in 10YO cyclist was 20 km/h or more.

It was found that HIC_{15} in both 10YO and AM50 cyclists exceeded the criterion even in the car speed of 10 km/h when the cyclists fell down toward the ground from his head.

ACKNOWLEDEMENT

The study used computational resources of the K computer provided by the RIKEN Advanced Institute for Computational Science through the HPCI System Research project as a part of the Japan Automotive Manufacture Association, Inc.'s research activities (Project ID: hp170150). The authors would like to appreciate the RIKEN Advanced Institute for Computational Science and the Fujitsu Limited.

REFERENCES

[1] National Police Agency in Japan, 2018.
[2] Vital Statistics in Japan, Ministry of Internal Affair and Communications Statistics Bureau, 2016.
[3] Ito, K., Tokuyama, M., Miyazaki, H., Hayashi, S., Kitagawa, Y., Yasuki, T. 2017. "Development of Child Finite Element (FE) Models and Vehicle-To-Pedestrian collision Simulations." 25th ESV, 17-0279.
[4] Takahashi, T., Fukushima, S., Kitagawa, Y., Yasuki, T. 2015."Injury Simulation of Rear Seat Child Occupant in Offset Deformable Barrier Frontal Impact." 24th ESV, 15-0048.
[5] Hamacher, M., Kuhn, M., Hummel, T., Eckstein, Lutz. 2017."Effectiveness of Pedestrian Safety Measures at the Vehicle Front with Regard to Cyclists." 25th ESV, 17-0177.
[6] Zander, O., Hamacher, M., 2017."Revison of Passive Pedestrian Test and Assessment Procedures to Implement Head Protection of Cyclists." 25th ESV, 17-0376.
[7] Maki, T., Kajzer, J., Mizuno, K., Sekine, Y. 2003. "Comparison of Vehicle-Bicycle and Vehicle-Pedestrian Accidents in Japan." Accident Analysis and Prevention, 35, 927-940.
[8] Omoda, Y., Konosu, A. 2016."Analysis of Bicyclists' Head Protection Methods during Head Impacts to a Car and the Ground in Bicyclist and Car Traffic Accidents, Using a Computer Simulation Analysis Method." JSAE, 47, 2, 20164189 (Japanese).
[9] Fahlstedt, M., Halldin, P., Alvarez, V.S., Kleiven, S. 2016. "Influence of the Body and Neck on Head Kinematics and Brain Injury Risk in Bicycle Accident Situations." IRCOBI Conference, IRC-16-64.
[10] Ito, D., Yamada, H., Oida, K., Mizuno, K. 2014. "Finite Element Analysis of Kinematics Behavior of Cyclist and Performance of Cyclist Helmet for Human Head Injury in Vehicle-to-Cyclist Collision." IRCOBI Conference, IRC-14-21.
[11] Katsuhara, T., Miyazaki, H., Kitagawa, Y., Yasuki, T. 2014. " Impact Kinematics of Cyclist and Head Injury Mechanism in Car-to-Bicycle Collision," IRCOBI Conference, IRC-14-76.
[12] Mertz, H.J., Prasad, P., Nusholtz, G. 1996. "Head Injury Risk Assessment for Forehead Impacts." SAE 960099, 26-46.
[13] Takhounts, E.G., Eppinger, R.H., Campbell, J.Q., Tannous, R.E., Power, E.D., Shook, L.S. 2003. "On the Development of the SIMon Finite Element Head Model." Stapp Car Crash Journal, 47, 107-133.
[14] Takounts, E.G., Craig, M.J., Moorhouse, K., McFadden, J., Hasija, V. 2013. "Development of Brain Injury Criteria (BrIC)." Stapp Car Crash Journal, 57, 243-266.
[15] Matsui, Y., Oikawa, S. 2015. "Feature of Fatal Cyclist Injury in Vehicle-Versus-Cyclist Accident in Japan." SAE, 2015-01-1415.